A Singularity-Analysis Approach to characterize Epicardial Electric Potential

Oriol Pont[1,2], Hussein Yahia[1], Rémi Dubois[2], Michel Haïssaguerre[2,3,4]

[1]Team GeoStat - INRIA Bordeaux Sud-Ouest,
Talence, France
[2]L'Institut de rythmologie et modélisation cardiaque LIRYC, Université de Bordeaux,
Bordeaux, France
[3]Centre de Recherche Cardio-Thoracique, Inserm U1045, Université Bordeaux Segalen,
Bordeaux, France
[4]CHU de Bordeaux, Hôpital Cardiologique du Haut-Lévêque,
Pessac, France

Abstract

The cardiac electrical activity conforms a complex system, for which nonlinear signal-processing is required to characterize it properly. In this context, an analysis in terms of singularity exponents is shown to provide compact and meaningful descriptors of the structure and dynamics. In particular, singularity components reconstruct the epicardial electric potential maps of human atria, inverse-mapped from surface potentials; such approach describe sinus-rhythm dynamics as well as atrial flutter and atrial fibrillation. We present several example cases in which the key descriptors in the form of fast-slow dynamics point at the arrhythmogenic areas in the atria.

1. Introduction

Specific nonlinear analysis methods are required to properly tackle the dynamics of the electrical activity of the human heart. Complex synchronization processes between pacemaker cells, conduction inhomogeneities and chaotic nonlinear amplification of fluctuations challenge descriptional efforts, especially those of forecasting value [1–4].

This is particularly crucial in complex arrhythmic regimes or at any level where linearizations deviate significantly from the described phenomena. In a context of noninvasive mapping of the epicardial potential, singularity analysis becomes an appropriate processing methodology that can provide robust and accurate characterizations of dynamical transition fronts [5–7].

In this work, we derive from first principles an effective cardiodynamical description where singularity exponents sift a simple fast dynamics from its slow modulation [8,9]. We characterize singularity transitions in epicardial potential maps from patients with atrial flutter and atrial fibrilla-

tion.

Such local transition analysis could eventually be incorporated to the inverse-problem regularization and improve information on anomalous activity areas to e.g., support diagnosis or guide catheter ablation procedures.

Atrial fibrillation (AF), the most common form of cardiac arrhythmia, consists in the chaotic operation, electrical activation and pumping of the atria. In some circumstances, it can induce life-threatening complications such as inducing a heart failure or forming blood clots that lead to stroke. In cases where medication is impossible or ineffective, a successful treatment consists in radiofrequency ablation of the endocardial tissue to ease an appropriate electrical conduction. In case of paroxysmal AF, Haïssaguerre et al. have shown [10] that for 80 % of patients, electrical insulation of the pulmonary veins allows the patient to regain a normal heart rhythm [11–17], but in persistent or permanent AF, the location of pathogen areas remains difficult and is still an open problem.

The paper is structured as follows: the next Section introduces the methods used for the signal processing. In Section 3 we present how in terms of signal reconstruction we are able to naturally define a way to sift a simple fast dynamics from a slow dynamical modulation over it. This is shown to provide meaningful descriptors of the analyzed cases of atrial arrhythmias. Finally, in Section 4 we draw the conclusions of our work.

2. Singularity analysis methods

The singularity degree of a point in a signal is conceptually linked to how rare or unreconstructible is the value at that point from the rest of the signal. A reconstruction kernel that is deterministic, linear, isotropic and translational invariant is uniquely defined and its form implies

locally evaluated singularities and thus no need to assume any kind of stationarity [6, 18, 19].

Basically, given a signal $s(\mathbf{x})$, we will say it has a singularity exponent $h(\mathbf{x})$ when the following equation holds:

$$\mathcal{T}_{\Psi}\mu(\mathbf{x}, r) = \alpha_{\Psi}(\mathbf{x})r^{h(\mathbf{x})} + o\left(r^{h(\mathbf{x})}\right) \qquad (r \to 0) \quad (1)$$

where $\mathcal{T}_{\Psi}\mu(\mathbf{x}, r) = \int_{\mathbb{R}} \mathrm{d}\mu(\mathbf{x}') \, \Psi\left((\mathbf{x} - \mathbf{x}')/r\right)$ is the wavelet projection of the measure μ at point $\mathbf{x}$ (spatial or temporal) and scale r, $\mathrm{d}\mu(\mathbf{x}) = \|\nabla s\|(\mathbf{x}) \, \mathrm{d}\mathbf{x}$ is the *gradient-modulus measure* and Ψ is a certain kernel known as *mother wavelet*.

2.1. Source field (SF)

As reported in [8, 9], the orientation of singularities defines a fast and simple dynamics which, for the case of heartbeat, is statistically compatible with a stochastic process without memory. The key manifold of the signal driving its dynamics is called the *oriented* most-singular component.

Reconstructing the signal by a reconstruction kernel [6] only from that oriented manifold results in a *reduced signal*, which follows the same behaviour (1) with the same exponents but different prefactor $\alpha(\mathbf{x})$ and secondary terms. The modulation factor linking the original with the reduced signal defines a complex but slow dynamics called source field (SF):

$$\mu_s(\mathcal{A}) = \int_{\mathcal{A}} \mathrm{d}\mu_r(\vec{x}, t) \, SF(\vec{x}, t) \qquad (2)$$

where r refers to the reduced signal. This allows defining the SF as the Radon-Nikodym derivative between the measure on the signal and that on the reduced signal,

$$SF(\vec{x}, t) = \frac{\mathrm{d}\mu_{\mathrm{s}}}{\mathrm{d}\mu_{\mathrm{r}}}(\vec{x}, t) \qquad (3)$$

3. Describing heart potential maps under atrial flutter and atrial fibrillation

As a preliminary analysis, we have processed epicardial electric potential signals for two patients who where treated with radio-frequency ablation at the Haut-Leveque hospital in Bordeaux. The recordings correspond to differences of electric potential between electrodes placed along a vest on the surface of the thorax. Previous to the recording, the heart geometry and its relative position to the electrodes is acquired, in order to perform an inverse mapping of the potential on the epicardial surface [20–22].

The two cases analyzed:
• P1: Male patient, 57 years old. First ablation for a common atrial flutter, consisting of counterclockwise reentry around the tricuspid valve. Ablation of this area resolved the arrhythmia.
• P2: Female patient, 73 years old. First ablation for a case of persistent atrial fibrillation (recurrent episodes which may last more than 7 days). At the beginning of the ablation procedure, an average atrial fibrillation cycle length of 200ms was measured on both left and right atrial appendages. A fragmented potential was found in posterior inferior left atrium. Ablation in this region converted the atrial fibrillation into atrial tachycardia. A second mapping confirmed a counterclockwise flutter in the right atrium, around the tricuspid valve.

The signal processed is the electric potential mapped on the surface of the atria. This corresponds to 11 489 time instances (1kHz sampling) each of a spatial map on a 1496-point atrial grid for P1, and 18647 maps of 1636 points for P2. Potential maps are reconstructed from inverting the body surface maps (ecVue, CardioInsight, Cleveland OH) [20]. In any case, we have canceled the QRS complexes as detected on the body surface ECGs, since the ventricular activity blinds a proper mapping on the atria; we have used an algorithm based to that in [23], improved and adapted to our case.

The robust and compact framework provided by the singularity exponents and source field can give a proper description while filtering spurious effects, in a model-agnostic way that stays as close to the empirical data as possible. The first step has been to validate that eq. (1) is verified in both space and time for our signals. This means that calculating singularity exponents makes sense in that case; the approach had been validated for endocardial potential [9] but only in the time domain. In the space domain, the estimation is done by considering the relative positions and orientations of the nearest neighbours.

The results are shown in Figure 1 for the case of atrial flutter P1 and Figure 2 for the case of atrial fibrillation P2. In both cases, the extreme values of singularity exponents and source field highlight areas specifically related to the arrhythmias. In case P1, the reentry around the valve is traduced in less regular exponents and higher value of SF, meaning larger modulation factor. The SF field changes more abruptly in the reentry region, showing more specifically the problem area. In case P2, a complex atrial fibrillation, the exponents in the arrhythmogenic areas are larger and the SF values are smaller, meaning a smaller modulation factor and so a larger role of the orientational dynamics. In that complex behaviour, key areas actually take opposite values to those of when there is a simple reentry. The sharper transitions characterized as smaller singularity exponents indicate the reentry area, but in the complex fibrillation it is the more persistent areas that perturb the normal operation. In a generic case, both extreme values can be indicating an arrhythmogenic point in the tissue.

Consistently in both cases, the SF behaves more specif-

ically in the edges of the areas, and also consistently the activations around the pulmonary veins have relatively smaller SF values, indicating a larger influence of the orientational dynamics [9] in them.
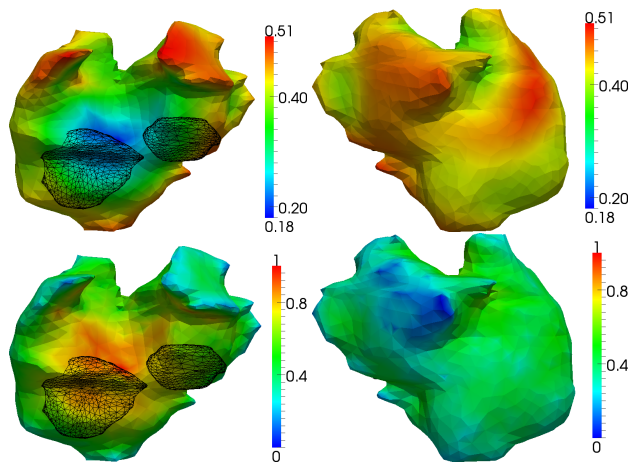

Figure 1. Median singularity exponent (top) and average normalized SF value (bottom) of the epicardial electric potential in a case of atrial flutter, patient P1. We show the mapping on the atria and indicate the position of the valves for reference. We observe a concentration of less regular exponents and larger source field in the key area around the tricuspid valve. The source field is more specific on the flutter area, also ignoring the fluctuations that the exponents show on the anterior area. Error propagations in the algorithms indicate a sigma around 0.03 for the exponents and 0.1 for the SF.

4. Discussion and conclusions

A noninvasive map sequence of epicardial potential allows evaluation of spatio-temporal singularity exponents in that signal. While the regular low-variation areas are more prone to be affected by masking artefacts of the inverse projections, the most singular points describing the transitions are expected to be comparatively less perturbed. This way spurious effects can be filtered out and working on the singularity field can be more robust than on the potential signal itself, while staying close to the physical data and without imposing any model or unreasonable hypothesis.

Moreover, introducing the source field SF that relates the actual signal to that derived from a measure of its singularity orientation provides a sharper and more specific descriptor of transitional dynamics. We have processed maps under atrial flutter and atrial fibrillation conditions, showing exponent and SF transitions connected to problem areas on the anomalous atrial cardiac dynamics. Prospectively, these transition descriptors could be used to help
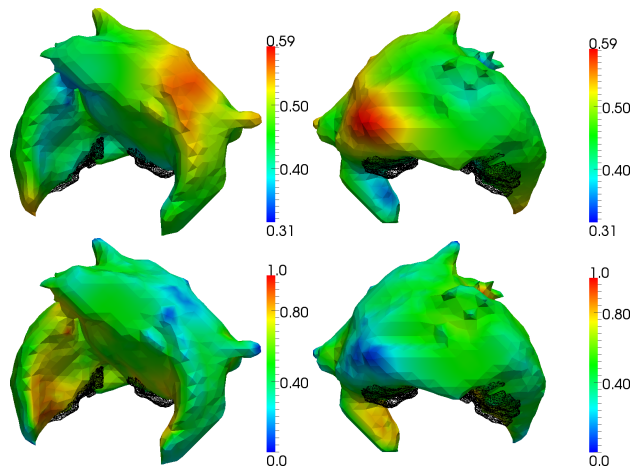

Figure 2. Median singularity exponent (top) and average SF value (bottom) of the epicardial electric potential in a case of atrial fibrillation, patient P2. We show the mapping on the atria and indicate the position of the valves for reference. Both fields highlight key fibrillation areas as the pulmonary veins and the left posterior inferior area whose ablation ended the fibrillation. The SF is more specific. Error propagations in the algorithms indicate a sigma around 0.03 for the exponents and 0.1 for the SF.

the regularization of the inverse mapping, also eventually provide indicators of anomalous activity areas that help as diagnosis or operation supports.

References

[1] Ivanov P, Amaral L, Goldberger A, Havlin S, Rosenblum M, Struzik Z, Stanley H. Multifractality in human heartbeat dynamics. Nature 1999;399:461–465.

[2] Ivanov P. Long-range dependence in heartbeat dynamics. In Rangarajan G, Ding M (eds.), Processes with Long-Range Correlations, volume 621 of Lecture Notes in Physics. Springer Berlin / Heidelberg, 2003; 339–372. 10.1007/3-540-44832-2.

[3] Kozaitis SP. Improved feature detection in ecg signals through denoising. International Journal of Signal and Imaging Systems Engineering 2008;1(2):108–114.

[4] Martinelli M, Moroni D, Salvetti O, Tampucci M. A knowledge-based infrastructure for the management of diagnostic imaging procedures in the heart failure domain. In

Transactions on Mass-Data Analysis of Images and Signals 2010;2: 3–18.

[5] Pont O, Turiel A, Pérez-Vicente CJ. Application of the microcanonical multifractal formalism to monofractal systems. Physical Review E 2006;74:061110–061123.

[6] Turiel A, Yahia H, Pérez-Vicente C. Microcanonical multifractal formalism: a geometrical approach to multifractal systems. Part I: Singularity analysis. Journal of Physics A 2008;41:015501.

[7] Pont O, Turiel A, Perez-Vicente C. Empirical evidences of a common multifractal signature in economic, biological and physical systems. Physica A 2009;388(10):2025–2035.

[8] Pont O, Haïssaguerre M, Yahia H, Derval N, Hocini M. Heartbeat dynamics from a microcanonical multifractal approach. In Computing in Cardiology 2011;38:705-708.

[9] Pont O, Haïssaguerre M, Yahia H, Derval N, Hocini M. Microcanonical processing methodology for ECG and intracardiac potential: application to atrial fibrillation. Transactions on Mass Data Analysis of Images and Signals 2012;4(1):19–38. URL http://hal.inria.fr/hal-00668550.

[10] Haïssaguerre M, Jaïs P, Shah DC, Takahashi A, Hocini M, Quiniou G, Garrigue S, Le Mouroux A, Le Métayer P, Clémenty J. Spontaneous initiation of atrial fibrillation by ectopic beats originating in the pulmonary veins. New England Journal of Medicine 1998;339(10):659–666. ISSN 0028-4793. URL http://dx.doi.org/10.1056/NEJM199809033391003.

[11] Dubois R, Roussel P, Hocini M, Sacher F, Haissaguerre M, Dreyfus G. A wavelet transform for atrial fibrillation cycle length measurements. In Computers in Cardiology 2009; 501 –504.

[12] Sanders P, Nalliah CJ, Dubois R, Takahashi Y, Hocini M, Rotter M, Rostock T, Sacher F, Hsu Lf, Jönsson A, O'neill MD, Jaïs P, Haïssaguerre M. Frequency mapping of the pulmonary veins in paroxysmal versus permanent atrial fibrillation. Journal of Cardiovascular Electrophysiology 2006;17(9):965–972. ISSN 1540-8167. URL http://dx.doi.org/10.1111/j.1540-8167.2006.00546.x.

[13] Takahashi Y, Sanders P, Jaïs P, Hocini M, Dubois R, Rotter M, Rostock T, Nalliah CJ, Sacher F, Clémenty J, Haïssaguerre M. Organization of frequency spectra of atrial fibrillation: Relevance to radiofrequency catheter ablation. Journal of Cardiovascular Electrophysiology 2006;17(4):382–388. ISSN 1540-8167. URL http://dx.doi.org/10.1111/j.1540-8167.2005.00414.x.

[14] Hocini M, Jais P, Sanders P, Takahashi Y, Rotter M, Rostock T, Hsu LF, Sacher F, Reuter S, Clementy J, Haissaguerre M. Techniques, evaluation, and consequences of linear block at the left atrial roof in paroxysmal atrial fibrillation: a prospective randomized study. Circulation 2005; 112(24):3688–3696.

[15] Hocini M, Sanders P, Jaïs P, Hsu LF, Weerasoriya R, Scavée C, Takahashi Y, Rotter M, Raybaud F, Macle L, Clémenty J, Haïssaguerre M. Prevalence of pulmonary vein disconnection after anatomical ablation for atrial fibrillation: consequences of wide atrial encircling of the pulmonary veins. European Heart Journal 2005;26(7):696–704. URL http://eurheartj.oxfordjournals.org/content/26/7/696.abstract.

[16] Hocini M, Jais P, Sacher F, Reuter S, Clementy J, Haissaguerre M. Mapping and ablation of malignant ventricular arrhythmias. Arch Mal Coeur Vaiss 2005;98(5):34–41. URL http://www.ncbi.nlm.nih.gov/pubmed/16433241.

[17] Haissaguerre M, Extramiana F, Hocini M, Cauchemez B, Jais P, Cabrera JA, Farre G, Leenhardt A, Sanders P, Scavee C, Hsu LF, Weerasooriya R, Shah DC, Frank R, Maury P, Delay M, Garrigue S, Clementy J. Mapping and ablation of ventricular fibrillation associated with long-qt and brugada syndromes. Circulation 2003;108(8):925–928. URL http://circ.ahajournals.org/cgi/content/abstract/108/8/925.

[18] Pont O, Turiel A, Perez-Vicente C. On optimal wavelet bases for the realization of microcanonical cascade processes. Int J Wavelets Multi IJWMIP 2011;9(1):35–61.

[19] Pont O, Turiel A, Yahia H. An optimized algorithm for the evaluation of local singularity exponents in digital signals. In Aggarwal J, Barneva R, Brimkov V, Koroutchev K, Korutcheva E (eds.), 14th International Workshop, IWCIA 2011, volume 6636 of Lecture Notes in Computer Science (LNCS). Madrid, Spain: Springer, 2011; 346–357. URL http://hal.inria.fr/inria-00581057/en/.

[20] Ramanathan C, Ghanem RN, Jia P, Ryu K, Rudy Y. Noninvasive electrocardiographic imaging for cardiac electrophysiology and arrhythmia. Nat Med 2004;10(4):422–428. ISSN 1078-8956. URL http://dx.doi.org/10.1038/nm1011.

[21] Jia P, Ramanathan C, Ghanem RN, Ryu K, Varma N, Rudy Y. Electrocardiographic imaging of cardiac resynchronization therapy in heart failure: Observation of variable electrophysiologic responses. Heart Rhythm 2006;3(3):296–310. ISSN 1547-5271. URL http://linkinghub.elsevier.com/retrieve/pii/S1547527105023593?showall=true.

[22] Cuculich PS, Wang Y, Lindsay BD, Faddis MN, Schuessler RB, Damiano RJ, Li L, Rudy Y. Noninvasive characterization of epicardial activation in humans with diverse atrial fibrillation patterns / clinical perspective. Circulation 2010;122(14):1364–1372. URL http://circ.ahajournals.org/content/122/14/1364.abstract.

[23] Stridh M, Sornmo L. Spatiotemporal qrst cancellation techniques for analysis of atrial fibrillation. IEEE Trans Biomed Eng 2001;48(1):105–111. 0018-9294 (Linking).

Address for correspondence:

Oriol Pont
oriol.pont@inria.fr